Bull. Chem. Soc. Jpn. Vol. 83, No. 3, 261–266 (2010)

Calorimetric Study of Correlated Ligand Dynamics in Mixed-Valence MMX Chain Complex [{Ni_2(*n*-BuCS_2)$_4$}I]

Satoaki Ikeuchi,[1,2,†] **Yasuhisa Yamamura,**[2] **Yuji Yoshida,**[3] **Minoru Mitsumi,**[3]
Koshiro Toriumi,[3] **and Kazuya Saito***[2]

[1]Department of Chemistry, Graduate School of Science, Osaka University, Toyonaka, Osaka 560-0043

[2]Department of Chemistry, Graduate School of Pure and Applied Sciences, University of Tsukuba, Tsukuba 305-8571

[3]Department of Material Science, University of Hyogo, Kouto, Kamigori-cho, Hyogo 678-1297

Received November 19, 2009; E-mail: kazuya@chem.tsukuba.ac.jp

Heat capacity of a mixed-valence complex having a one-dimensional chain structure, [{Ni_2(*n*-BuCS_2)$_4$}I] (*n*-Bu = butyl group), was measured between 10 and 325 K by adiabatic calorimetry. Anomalies due to phase transitions were detected around 135 and 260 K. The anomaly around 260 K was of multiple-peaks. The excess entropy acquired below the phase transition around 260 K is much smaller than the simple estimate based on the structural disorder found in the crystal structure, implying the presence of motional correlation in dynamics of *n*-BuCS_2 ligands. Through the comparison with the corresponding Pt complex, [{Pt_2(*n*-BuCS_2)$_4$}I], the phase transition around 135 K is also discussed in relation to the absence in the present complex of a spin-Peierls transition observed in other members of Ni complexes with similar chain structures.

Molecules and/or atomic groups are, even in crystalline state, perpetually in motion, which includes not only small amplitude (harmonic) vibration but also large amplitude motion such as reorientation. Molecular dynamics, which usually refer to the latter, have been investigated by utilizing a wide variety of spectroscopies. Because of difficulties, however, it is often the case where the experimental results are analyzed in a single-particle scheme within the mean field spirit. On the other hand, it is quite certain that many interesting phenomena in condensed matter are brought about by correlation effects. It is therefore highly desired to explore the correlated molecular dynamics. In this paper, a clear symptom of motional correlation in ligand dynamics is identified in the crystal of a mixed-valence one-dimensional complex, [{Ni_2(*n*-BuCS_2)$_4$}I]. In this context, this paper is an extension of our study utilizing (absolute) calorimetry of correlated dynamics.[1–5] Enumeration of entropy by calorimetry is crucially important in the study of correlation effects because the entropy directly senses the number of microscopic states through the Boltzmann principle.

Mixed-valence complexes with one-dimensional (1D) structure represented as –M–M–X– (M, metal ion; X, halogen ion) have attracted much attention because of the possible variety in electronic/magnetic states.[6–11] Besides the possible variety in electronic/magnetic orders, the ligands in MMX complexes play an important role beyond those of a simple spacer, charge compensator, and chemical stabilizer. In a series of –Pt–Pt–I– complexes, the dynamics of ligands (RCS_2, R = alkyl group) strongly affects the electronic/magnetic properties.[12–14] For example, the phase transition from a magnetic (antiferromagnetically interacting) state to a non-magnetic state occurs while accompanying structural ordering of the ligands in [{Pt_2(*n*-PrCS_2)$_4$}I] and [{Pt_2(*n*-BuCS_2)$_4$}I], at least in the former of which both changes proceed simultaneously and gradually.[12] Besides, a similar complex with hexyl groups, [{Pt_2(*n*-HexCS_2)$_4$}I], exhibits physical properties far from the trend observed in shorter alkyl groups.[14] This implies that the interplay between electronic and motional degrees of freedom is relevant for their electronic states due to their structural complexity.

In this paper, a MMX complex with Ni ions [{Ni_2(*n*-BuCS_2)$_4$}I],[15] is dealt with. The change of metal ions from Pt to Ni mainly affects the tendency of localization of unpaired electrons.[7,8,16–19] Indeed, the Ni complexes (R = Et, *n*-Pr, and *n*-Bu) are insulating and reasonably described by a 1D antiferromagnetic chain model[15,20] whereas the Pt complexes are metallic or semiconducting around room temperature.[8,21,22] We have studied properties of MMX complexes in detail[1,12–14,20,23] in the course of a comprehensive study on the interplay between electronic and motional degrees of freedom.[24–31] Our systematic study has revealed that the Pt complexes exhibit notable interplay depending on the length of alkyl groups in ligands as described above, whereas direct coupling with ligand dynamics is not significant in the Ni complexes. Indeed, in [{Ni_2(*n*-PrCS_2)$_4$}I], the ordering of ligands takes place at 205.6 K independently with the magnetic (spin-Peierls) transition around 40 K.

The crystal structure of [{Ni_2(*n*-BuCS_2)$_4$}I] has been determined as shown in Figure 1 at room temperature.[15] Although the space group (*P*4/*m*) is different from that of the corresponding Pt complex, [{Pt_2(*n*-BuCS_2)$_4$}I] (*I*4/*m*),[22] their structures are very similar to each other. The period along

---

[†] Present address: ULVAC Riko, 1-9-19 Hakusan, Midori-ku, Yokohama 226-0006.

Published on the web February 26, 2010; doi:10.1246/bcsj.20090301

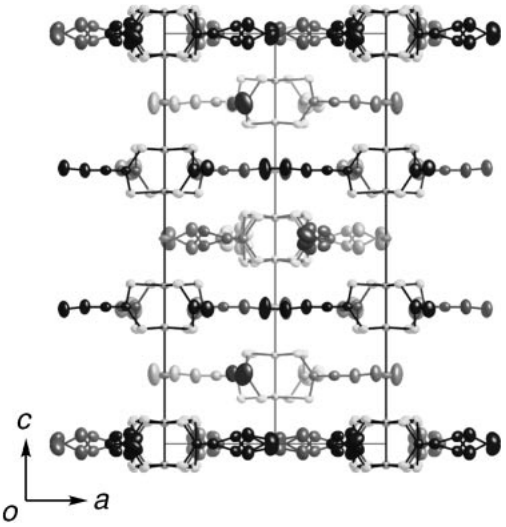

Figure 1. Unit cell of [{Ni$_2$(*n*-BuCS$_2$)$_4$}I] at room temperature viewed along the *b* axis. The central MMX chain (along the *c* axis) located at the center of the *ab*-plane shows the sequence of –left–disorder–right– concerning the twist of the CS$_2$ groups with increasing *z* (upward). The chains located at the edges show the same sequence starting from the disordered CS$_2$ group.

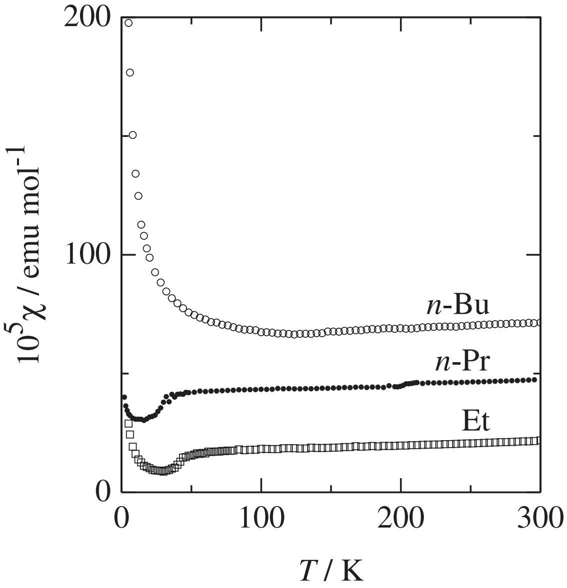

Figure 2. Magnetic susceptibilities of [{Ni$_2$(RCS$_2$)$_4$}I] (R = Et, *n*-Pr, and *n*-Bu) measured upon cooling from room temperature. Data are shifted upward by 25×10^{-5} emu mol^{-1} for R = *n*-Pr and by 50×10^{-5} emu mol^{-1} for R = *n*-Bu. The sudden decrease in magnetic susceptibility of R = Et and *n*-Pr is due to spin-Peierls transitions.

the *c* axis is tripled in the unit of –M–M–X–. This periodicity describes the structural disorder concerning the CS$_2$ and butyl groups. Four CS$_2$ groups belonging to the two ordered complexes are twisted right or left. The linear chain structure is represented by the twisted manner of [{Ni$_2$(*n*-BuCS$_2$)$_4$}I] units as a sequence of –right–disorder–left– as seen in Figure 1. The magnetic susceptibility at room temperature was reported to be a similar magnitude to those of other Ni complexes as shown in Figure 2, suggesting the antiferromagnetic coupling between localized spins on the MMX unit.[15] On cooling from room temperature, the magnetic susceptibility increases below 100 K and diverges at low temperatures. This increase in magnetic susceptibility is difficult to explain while assuming merely the contribution of impurity spin when compared with those of other Ni complexes as seen in Figure 2. Since the structural disorder at room temperature is similar to that of [{Pt$_2$(*n*-BuCS$_2$)$_4$}I],[22] a similar phase transition is expected below room temperature. The present study reveals the existence of a phase transition at 135 K, which destroys the potential spin-Peierls order at low temperatures.

Experimental

[{Ni$_2$(*n*-BuCS$_2$)$_4$}I] was synthesized according to a method described elsewhere.[15] Since the sample (consisting of a vast number of tiny crystals) is slightly hygroscopic, it was loaded into a gold-plated copper calorimeter vessel under nitrogen atmosphere. The vessel filled with nitrogen gas was evacuated for about 1 h and pinched off after introducing helium gas (10^5 Pa at room temperature) for assisting thermal equilibration inside the vessel. The amount of the sample was determined as the difference in mass of the vessel with and without the sample. The buoyancy correction yielded the mass of the sample as 1.8278 g.

The working thermometer attached to the calorimeter vessel was a platinum resistance thermometer (Minco, S1059). Its temperature scale is based upon the ITS-90. The details of the adiabatic calorimeter used and its operations are described elsewhere.[32]

The measurement was carried out by adiabatic intermittent heating. The temperature increment by a single energy input (Joule heating) was less than 1% of temperature. Thermal equilibrium inside the vessel was attained within a normal time (1–10 min depending on temperature) after energy input was turned off. The sample contributed to heat capacity by 17% of the total heat capacity including that of the vessel at 50 K, 14% at 100 K, 16% at 200 K, 20% at 300 K, and 21% at 325 K.

Results and Discussion

Thermal Stability and Phase Transitions. The heat capacity of [{Ni$_2$(*n*-BuCS$_2$)$_4$}I] was measured between 10 and 325 K, above which the sample decomposed as evidenced by strong heat evolution. Typical results are shown in Figure 3 for the whole temperature range studied. Thermal anomalies are detected around 245, 260, and 270 K as seen in Figure 3. The data around these anomalies are shown in Figure 4 in an enlarged scale. The data plotted by circles were obtained in a measurement starting from 189 K in the heating direction, whereas the data shown by pluses from 258.5 K, which is 1.5 K lower than 260 K. On the other hand, the data shown by crosses were obtained in a measurement starting after heating from 227.7 to 251.8 K and cooling down to 242.5 K, which is 2.5 K lower than the lowest temperature among the three anomalies, 245 K. The observed supercooling phenomena clearly show that the phase transitions are of the first order.

Since the temperatures of these anomalies are different from those of melting of *n*-hexane and benzene used as solvents for recrystallization in sample preparation, they are of the Ni complex. It is noted that only an anomaly was detected in the temperature dependence of magnetic susceptibility in this

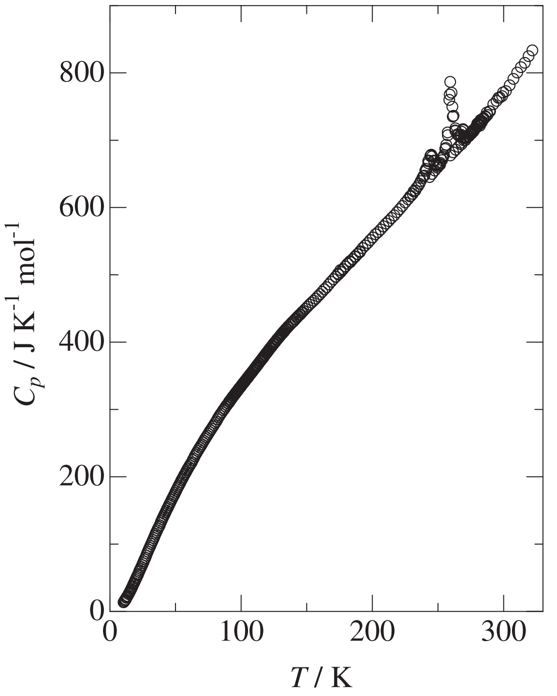

Figure 3. Measured heat capacities of [{$Ni_2(n\text{-}BuCS_2)_4$}I].

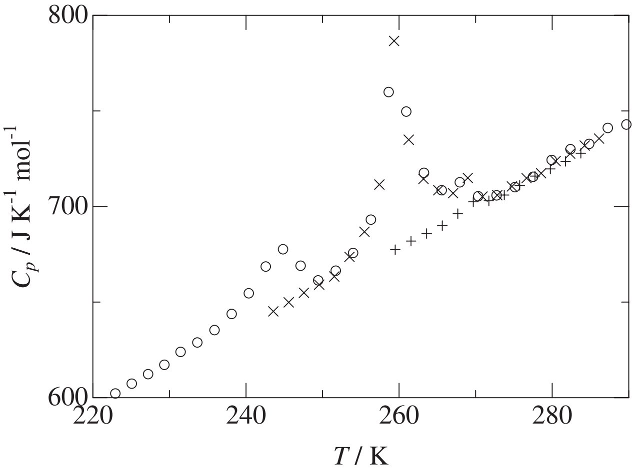

Figure 4. Measured heat capacities of [{$Ni_2(n\text{-}BuCS_2)_4$}I] around the MT–RT phase transition. The data obtained in separate runs are distinguished by different symbols.

temperature region.[15] As the sample used was synthesized in three batches, these anomalies may be related to each batch. From now on, three anomalies at 250, 260, and 270 K are treated as a united anomaly corresponding to a phase transition between the middle-temperature (MT) phase and the room-temperature (RT) phase.

Beside sharp anomalies at high temperatures, a broad anomaly is observed around 135 K as seen in Figure 5a. The location is reasonably close to the temperature of the weak anomaly detected in the magnetic study[15] seen in Figure 2. Since no latent heat was detected, this anomaly is attributed to a higher-order phase transition. The phase below this phase transition is designated as the low-temperature (LT) phase hereafter.

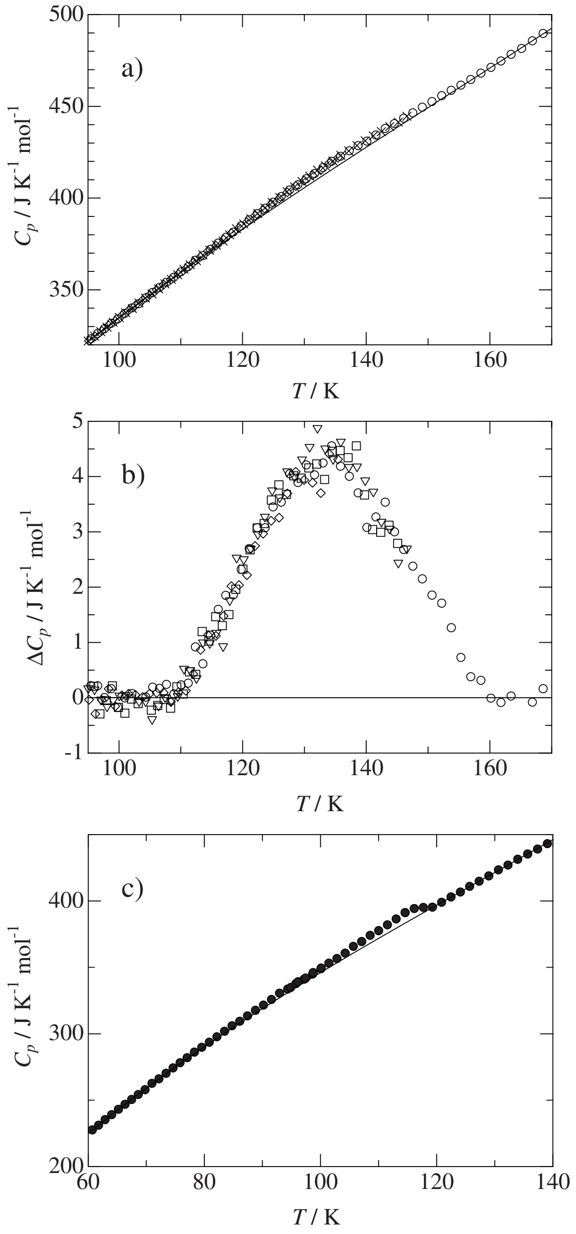

Figure 5. Measured heat capacities around the LT–MT phase transition of [{$Ni_2(n\text{-}BuCS_2)_4$}I] (a) and of [{$Pt_2(n\text{-}BuCS_2)_4$}I][13] (c), and the excess heat capacities due to the phase transition for [{$Ni_2(n\text{-}BuCS_2)_4$}I] (b) assuming the normal heat capacity drawn by a solid line in (a).

To see the magnitude and the shape of the anomaly around 135 K, a baseline of the heat capacity was assumed to be a smooth interpolating curve between 95 and 170 K. In practice, the baseline was approximated by a cubic polynomial as shown by a solid curve in Figure 5a. The excess heat capacity was then determined by subtracting the normal portion from the experimental data as shown in Figure 5b, where the data obtained in different series of measurements are plotted by different symbols. The integration of the excess heat capacity yields the excess enthalpy and entropy as about 126 J mol^{-1} and 0.95 J K^{-1} mol^{-1}, respectively.

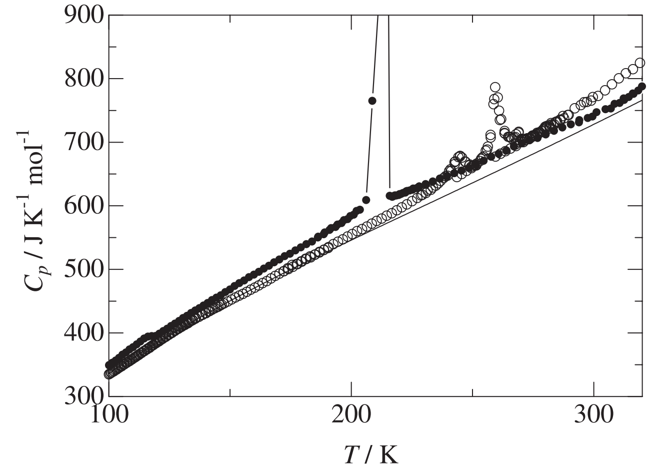

Figure 6. Heat capacities of $[\{Ni_2(n\text{-}BuCS_2)_4\}I]$ (open circle) and of $[\{Pt_2(n\text{-}BuCS_2)_4\}I]$ (filled circle). A normal heat capacity for $[\{Ni_2(n\text{-}BuCS_2)_4\}I]$ estimated as the sum of heat capacities of $[\{Ni_2(n\text{-}PrCS_2)_4\}I]$ and polyethylene is drawn by a solid line.

Structural Disorder and Correlation in Ligand Dynamics. The crystal structure of $[\{Ni_2(n\text{-}BuCS_2)_4\}I]$ has been determined only for the RT phase.[15] Although there is no information on its crystal structure, it seems natural to assume the LT phase being ordered because neither phase transition nor glass transition was detected, implying that the LT phase obeys the third-law of thermodynamics. Since the LT–MT phase transition is expected to be of displacive type, the entropy due to structural disorder is reasonably assumed as null for the MT phase too.

The excess entropy involved in three anomalies around 260 K is much smaller than the expected entropy calculated by the model of structural disorder (ca. 15.4 J K^{-1} mol^{-1}), which works quite well for the corresponding phase transitions in $[\{Pt_2(n\text{-}PrCS_2)_4\}I]$ and of $[\{Pt_2(n\text{-}BuCS_2)_4\}I]$.[12,13] Since the model assumes no correlation in the ligand dynamics, the disagreement suggests that the strong correlation is active.

Around room temperature, in spite of its smaller molar mass, the heat capacity of $[\{Ni_2(n\text{-}BuCS_2)_4\}I]$ is definitely larger than that of $[Pt_2(n\text{-}BuCS_2)_4]I]$ as shown in Figure 6. Such a tendency is not found between $[\{Ni_2(n\text{-}PrCS_2)_4\}I]$ and $[\{Pt_2(n\text{-}PrCS_2)_4\}I]$.[12,20] The different behavior can be rationalized if the heat capacity of $[\{Ni_2(n\text{-}BuCS_2)_4\}I]$ around room temperature involves the significant contribution due to the thermal excitation of structural disorder. To estimate the excess heat capacity due to thermal evolution of the structural disorder, a baseline for $[\{Ni_2(n\text{-}BuCS_2)_4\}I]$ was tentatively assumed as the sum of the heat capacities of $[\{Ni_2(n\text{-}PrCS_2)_4\}I]$[20] and polyethylene.[33] The baseline thus assumed is shown in Figure 6. The excess heat capacity of $[\{Ni_2(n\text{-}BuCS_2)_4\}I]$ was then estimated as the difference between the experimental heat capacity and this baseline. The resultant excess heat capacities are shown in Figure 7a. The excess heat capacity is effectively null below 160 K, implying that the structural disorder of the ligands is excited above 160 K.

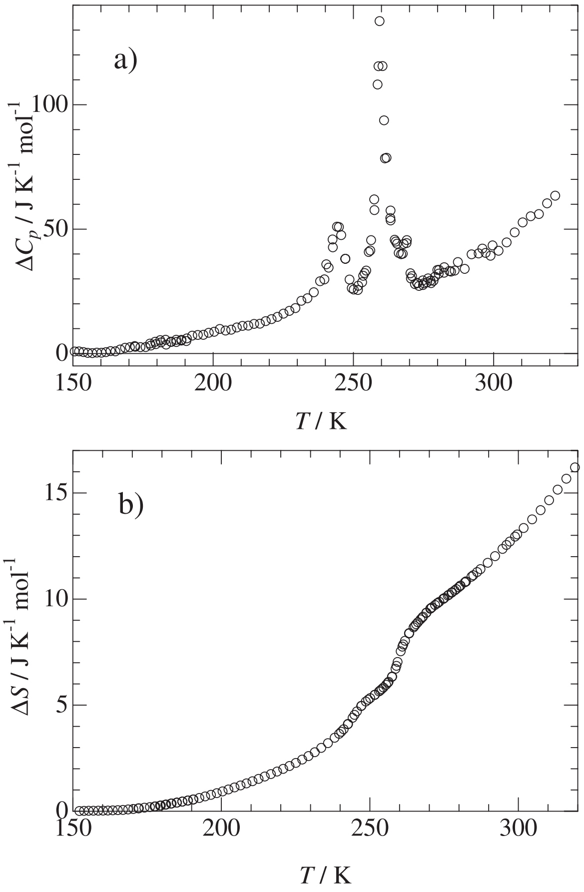

Figure 7. Excess heat capacities (a) and entropies (b) of $[\{Ni_2(n\text{-}BuCS_2)_4\}I]$ due to thermal excitation of structural disorder of the ligands.

The integration of the excess heat capacity above 160 K yields the excess enthalpy and entropy. The temperature dependence of the excess entropy above 160 K is shown in Figure 7b. The entropy increment between 160 and 260 K, which is the temperature of the main peak in heat capacity around the MT–RT phase transition, is about 9 J K^{-1} mol^{-1}. This magnitude of excess entropy is still much smaller than that calculated from the model of structural disorder established for $[\{Pt_2(n\text{-}PrCS_2)_4\}I]$ and $[\{Pt_2(n\text{-}BuCS_2)_4\}I]$,[12,13] which assumes that both CS_2 and alkyl groups are independently disordered in one-third complexes in the RT phase. On the other hand, if four ligands are independently disordered with the perfect correlation between the CS_2 and alkyl moieties within a ligand, the entropy due to the change in structural disorder is calculated as $(1/3)R\ln 2^4$ ($\approx$7.68 J K^{-1} mol^{-1}). This estimate is the minimum magnitude physically acceptable and compared favorably with the experimental excess entropy. It is noted that the minimum transition entropy necessary to establish the symmetry determined crystallographically is $(1/3)R\ln 2$ ($\approx$1.92 J K^{-1} mol^{-1}). The larger magnitude of the excess entropy shown in Figure 7b is therefore compatible with the structural information.

It is natural to suppose that the smaller excess entropy than the estimate assuming the independent disordering reflects the correlation effects of the dynamics of ligands in the RT phase as reported in [{$Pt_2(MeCS_2)_4$}I].[1] The presence of the excess heat capacity in the RT phase implies that the motional correlation between the CS_2 and alkyl moieties within a ligand gradually disappears upon heating. Around room temperature, the excess entropy is comparable to the calculated entropy of transition [$(1/3)R\ln 2^4\cdot2^4 \approx 15.4\,\mathrm{J\,K^{-1}\,mol^{-1}}$] from the model of disorder established for [{$Pt_2(n\text{-}PrCS_2)_4$}I] and [{$Pt_2(n\text{-}BuCS_2)_4$}I].[12,13] The degree of disorder of the ligands in [{$Ni_2(n\text{-}BuCS_2)_4$}I] is effectively the same as those of [{$Pt_2(n\text{-}PrCS_2)_4$}I] and [{$Pt_2(n\text{-}BuCS_2)_4$}I] at room temperature. In this respect, it may be said that [{$Ni_2(n\text{-}BuCS_2)_4$}I] probably has HT phase similar to the Pt complexes,[12,13,23] but decomposes below the expected transition temperature.

There remains an issue to be considered. That is why the motional correlation is effective in the RT phase of [{$Ni_2(n\text{-}BuCS_2)_4$}I] while not in [{$Pt_2(n\text{-}BuCS_2)_4$}I][13] in spite of the close similarity in molecular and crystal structures. Although the crystal structure is similar, the space group ($P4/m$) of the RT phase of [{$Ni_2(n\text{-}BuCS_2)_4$}I][15] is different from that ($I4/m$) of the corresponding Pt complex[22] showing no effects of motional correlation. Besides, the structure is slightly different from the Pt complex as evidenced by the smaller lattice constants. This is contrary to the naive expectation that the interchain distance be longer in Ni compounds as found for [{$Ni_2(n\text{-}PrCS_2)_4$}I] and [{$Pt_2(n\text{-}PrCS_2)_4$}I].[15,22] The ionic radius is smaller for Ni ion than Pt ion. The repeat distance along the chain is smaller in [{$Ni_2(n\text{-}BuCS_2)_4$}I] than [{$Pt_2(n\text{-}BuCS_2)_4$}I], accordingly. Since the butyl group has a definite volume, the interchain distance should be longer in [{$Ni_2(n\text{-}BuCS_2)_4$}I] than in [{$Pt_2(n\text{-}BuCS_2)_4$}I]. The smaller lattice constants implies that the available space for the butyl group in [{$Ni_2(n\text{-}BuCS_2)_4$}I] is smaller than that in [{$Pt_2(n\text{-}BuCS_2)_4$}I]. The smaller space is surely unfavorable for independent dynamics. Therefore, the appearance of motional correlation in [{$Ni_2(n\text{-}BuCS_2)_4$}I] would originate in the following two factors: the difference in the space group of the RT phase and that in the free space available for the butyl group resulting from the slight difference in crystal packing. It is noted that the molecular dynamics in molecular crystals has long been studied and discussed within a single-particle scheme. The experimental detection of any manifestation of correlation effects is to be considered as an important step for full understanding of molecular dynamics in molecular crystals.

Defects and Suppression of Spin-Peierls Transition. The temperature and magnitude of entropy of LT–MT phase transition in [{$Ni_2(n\text{-}BuCS_2)_4$}I] resembles those in [{$Pt_2(n\text{-}BuCS_2)_4$}I][22] in Figure 5c. Because the alkyl chain length of [{$Ni_2(n\text{-}BuCS_2)_4$}I] is the same as that of [{$Pt_2(n\text{-}BuCS_2)_4$}I], the LT–MT phase transition of [{$Ni_2(n\text{-}BuCS_2)_4$}I] is expected to share the mechanism with [{$Pt_2(n\text{-}BuCS_2)_4$}I], though their structures at low temperatures have not fully been established.[15,22] Since the phase transition in [{$Pt_2(n\text{-}BuCS_2)_4$}I] occurs in nonmagnetic, insulating states without structural disorder, it is plausible that the LT–MT phase transition of [{$Ni_2(n\text{-}BuCS_2)_4$}I] is also displacive originating in the lattice degree of freedom. This is consistent with the small magnitude of the magnetic anomaly.

The entropy of the LT–MT phase transition of [{$Ni_2(n\text{-}BuCS_2)_4$}I] ($0.95\,\mathrm{J\,K^{-1}\,mol^{-1}}$) is much smaller than $R\ln 2$ ($\approx 5.8\,\mathrm{J\,K^{-1}\,mol^{-1}}$), a typical magnitude of the entropy of transition for an order–disorder phase transition. This implies that the LT–MT phase transition is displacive assuming that it purely originates in the lattice degree(s) of freedom.

The magnitude of magnetic susceptibility[15] above 150 K is reasonably explained by the 1D antiferromagnetic model (Bonner–Fisher model[34]), while that below 130 K deviates clearly from the model. On further cooling, at low temperatures the magnetic susceptibility diverges like that of paramagnetic spins as seen in Figure 2. The concentration of the paramagnetic spin is estimated to be about 2% from the diverging component of the magnetic susceptibility below 50 K. This concentration is much larger by one order of magnitude than the impurity spin concentration (about 0.2%) observed in other MMX complexes.[15,21,22]

Upon the LT–MT phase transition, some structural defects are unavoidably created in the 1D chain as domain walls. It is natural to assume that the structural defects accompany magnetic moments due to the paramagnetic nature of the MT phase even if the LT–MT phase transition purely originates in the structural degree(s) of freedom. The higher concentration of "impurity" spins in [{$Ni_2(n\text{-}BuCS_2)_4$}I] is thus explained as a natural consequence of the LT–MT phase transition.

The spin-Peierls transition occurs around 40 K in [{$Ni_2(EtCS_2)_4$}I] and [{$Ni_2(n\text{-}PrCS_2)_4$}I],[15,20] while no change to nonmagnetic state occurs below the LT–MT phase transition in the present complex. It is well known that the spin-Peierls system is highly sensitive to impurities and external pressure. For example, the significant effects of nonmagnetic impurities on the spin-Peierls system were reported for a typical compound, $CuGeO_3$.[35] The spin-Peierls state collapses in the crystal where Zn ion at 3% is substituted for Cu ion. Besides, by gentle pressure upon making a compacted pellet, the spin-Peierls transitions in $(DMe\text{-}DCNQI)_2Ag$ and $(DMe\text{-}DCNQI)_2Li$ disappear.[36] The disappearance of the spin-Peierls order in [{$Ni_2(n\text{-}BuCS_2)_4$}I] seems to be related to the inhomogeneous formation of structural/magnetic defects. It is interesting to note that the concentration of defects estimated from the magnetic susceptibility is comparable to the "critical concentration" of defects in $CuGeO_3$.[35] In contrast to $CuGeO_3$, however, the destruction of the spin-Peierls order in [{$Ni_2(n\text{-}BuCS_2)_4$}I] is caused by the intrinsic lattice instability. This is a striking characteristic of the destruction of spin-Peierls order in the present system.

Conclusion

The heat capacity of [{$Ni_2(n\text{-}BuCS_2)_4$}I] was measured between 10 and 325 K by adiabatic calorimetry. Anomalies were detected around 135 and 260 K. The anomaly around 260 K was of multiple-peaks. The excess entropy acquired below the phase transition around 260 K is much smaller than the simple estimate based on the structural disorder found in the crystal structure, implying the presence of motional correlation in dynamics of the ligands. The magnitude of the excess entropy is compatible with almost perfect correlation between the CS_2 and butyl moieties within a ligand. The phase transition around 135 K is of higher order and is displacive. It introduces into the LT phase the structural/magnetic defects, which destroy the spin-Peierls order appearing in other Ni complexes.

One of the authors (S.I.) expresses thanks for the center of excellence (21COE) program "Creation of Integrated EcoChemistry of Osaka University" for financial support.

References

1 Y. Miyazaki, Q. Wang, A. Sato, K. Saito, M. Yamamoto, H. Kitagawa, T. Mitani, M. Sorai, *J. Phys. Chem. B* **2002**, *106*, 197.

2 Y. Yamamura, T. Tsuji, K. Saito, M. Sorai, *J. Chem. Thermodyn.* **2004**, *36*, 525.

3 K. Saito, Y. Yamamura, *Thermochim. Acta* **2005**, *431*, 21.

4 Y. Yamamura, H. Saitoh, M. Sumita, K. Saito, *J. Phys.: Condens. Matter* **2007**, *19*, 176219.

5 Y. Yamamura, H. Shimoi, M. Sumita, S. Yasuzuka, K. Adachi, A. Fuyuhiro, S. Kawata, K. Saito, *J. Phys. Chem. A* **2008**, *112*, 4465.

6 C.-M. Che, F. H. Herbstein, W. P. Schaefer, R. E. Marsh, H. B. Gray, *J. Am. Chem. Soc.* **1983**, *105*, 4604.

7 C. Bellitto, A. Flamini, L. Gastaldi, L. Scaramuzza, *Inorg. Chem.* **1983**, *22*, 444.

8 H. Kitagawa, N. Onodera, J.-S. Ahn, T. Mitani, K. Toriumi, M. Yamashita, *Synth. Met.* **1997**, *86*, 1931.

9 S. Yamamoto, *Phys. Rev. B* **2001**, *63*, 125124.

10 M. Kuwabara, K. Yonemitsu, *J. Phys. Chem. Solids* **2001**, *62*, 435.

11 M. Yamashita, S. Takaishi, A. Kobayashi, H. Kitagawa, H. Matsuzaki, H. Okamoto, *Coord. Chem. Rev.* **2006**, *250*, 2335.

12 S. Ikeuchi, K. Saito, Y. Nakazawa, M. Mitsumi, K. Toriumi, M. Sorai, *J. Phys. Chem. B* **2004**, *108*, 387.

13 S. Ikeuchi, K. Saito, Y. Nakazawa, A. Sato, M. Mitsumi, K. Toriumi, M. Sorai, *Phys. Rev. B* **2002**, *66*, 115110.

14 S. Ikeuchi, Y. Yamamura, M. Mitsumi, K. Toriumi, H. Saitoh, T. Atake, K. Saito, *Chem. Lett.* **2009**, *38*, 1190.

15 M. Mitsumi, Y. Yoshida, A. Kohyama, Y. Kitagawa, Y. Ozawa, M. Kobayashi, K. Toriumi, M. Tadokoro, N. Ikeda, M. Okumura, M. Kurmoo, *Inorg. Chem.* **2009**, *48*, 6680.

16 Y. Wada, T. Mitani, K. Toriumi, M. Yamashita, *J. Phys. Soc. Jpn.* **1989**, *58*, 3013.

17 K. Iwano, K. Nasu, *J. Phys. Soc. Jpn.* **1992**, *61*, 1380.

18 S. M. Weber-Milbrodt, J. T. Gammel, A. R. Bishop, E. Y. Loh, Jr., *Phys. Rev. B* **1992**, *45*, 6435.

19 H. Okamoto, Y. Shimada, Y. Oka, A. Chainani, T. Takahashi, H. Kitagawa, T. Mitani, K. Toriumi, K. Inoue, T. Manabe, M. Yamashita, *Phys. Rev. B* **1996**, *54*, 8438.

20 S. Ikeuchi, Y. Yamamura, Y. Yoshida, M. Mitsumi, K. Toriumi, K. Saito, *J. Phys. Soc. Jpn.* **2009**, *78*, 094704.

21 M. Mitsumi, S. Umebayashi, Y. Ozawa, K. Toriumi, H. Kitagawa, T. Mitani, *Chem. Lett.* **2002**, 258.

22 M. Mitsumi, K. Kitamura, A. Morinaga, Y. Ozawa, M. Kobayashi, K. Toriumi, Y. Iso, H. Kitagawa, T. Mitani, *Angew. Chem., Int. Ed.* **2002**, *41*, 2767.

23 K. Saito, S. Ikeuchi, Y. Nakazawa, A. Sato, M. Mitsumi, T. Yamashita, K. Toriumi, M. Sorai, *J. Phys. Chem. B* **2005**, *109*, 2956.

24 K. Saito, H. Akutsu, M. Sorai, *Solid State Commun.* **1999**, *111*, 471.

25 K. Saito, Y. Yamamura, H. Kitagawa, D. Yoshida, T. Mitani, M. Sorai, *J. Phys. Soc. Jpn.* **1999**, *68*, 3592.

26 H. Akutsu, K. Saito, M. Sorai, *Phys. Rev. B* **2000**, *61*, 4346.

27 K. Saito, M. Okada, H. Akutsu, M. Sorai, *Chem. Phys. Lett.* **2000**, *318*, 75.

28 A. Sato, H. Akutsu, K. Saito, M. Sorai, *Synth. Met.* **2001**, *120*, 1035.

29 K. Saito, S. Ikeuchi, A. Ota, H. Yamochi, G. Saito, *Chem. Phys. Lett.* **2005**, *401*, 76.

30 K. Saito, M. Okada, H. Akutsu, A. Sato, M. Sorai, *J. Phys. Chem. B* **2004**, *108*, 1314.

31 S. Ikeuchi, Y. Miyazaki, S. Takeda, T. Akutagawa, S. Nishihara, T. Nakamura, K. Saito, *J. Chem. Phys.* **2005**, *123*, 044514.

32 Y. Yamamura, K. Saito, H. Saitoh, H. Matsuyama, K. Kikuchi, I. Ikemoto, *J. Phys. Chem. Solids* **1995**, *56*, 107.

33 S.-S. Chang, *J. Res. Natl. Bur. Stand., Sect. A.* **1976**, *A80*, 51.

34 J. C. Bonner, M. E. Fisher, *Phys. Rev.* **1964**, *135*, A640.

35 M. Hase, I. Terasaki, Y. Sasago, K. Uchinokura, H. Obara, *Phys. Rev. Lett.* **1993**, *71*, 4059.

36 Y. Nakazawa, A. Sato, M. Seki, K. Saito, K. Hiraki, T. Takahashi, K. Kanoda, M. Sorai, *Phys. Rev. B* **2003**, *68*, 085112.